

Cite this: *Analyst*, 2012, **137**, 4644

www.rsc.org/analyst

Functionalized shell-isolated nanoparticle-enhanced Raman spectroscopy for selective detection of trinitrotoluene†

Kai Qian, Honglin Liu, Liangbao Yang* and Jinhui Liu*

Received 11th July 2012, Accepted 8th August 2012

DOI: 10.1039/c2an35947b

Shell-isolated nanoparticle-enhanced Raman spectroscopy (SHINERS), which acts as the next generation of advanced spectroscopy, expands the versatility of surface-enhanced Raman spectroscopy (SERS). Here we present a facile one-step method to prepare functionalized core-shell nanoparticles for selective detection of trinitrotoluene (TNT) through the formation of Meisenheimer complexes. A well-designed type of tunable poly-(2-aminothiophenol) (PAT) shells on gold nanoparticles was prepared for the first time and the shell thickness of 2 nm could be controlled by only adjusting the molar ratio of sodium dodecylsulfate (SDS) to 2-aminothiophenol. The polymer shells shows prominent advantages, including uniformity, better chemical stability, being free of pin-holes and amino-functionalized.

Recently, using a very elegant approach Tian and co-workers have developed a “shell-isolated nanoparticle-enhanced Raman spectroscopy” based system known as SHINERS,¹ in which the Raman signal amplification is provided by gold nanoparticles with an ultrathin silica or alumina shell. The main virtue of SHINERS is that it conforms to different contours of samples while protecting the SERS-active nanostructure from contact with what is being probed and its vast number of practical applications involving various materials with diverse and much higher detection sensitivity.^{1,2} SHINERS acts as the next generation of advanced spectroscopy³ which has tremendous potential for use as a versatile molecular vibration spectroscopy to study structurally well-defined surfaces of diverse materials widely used in surface science, life sciences, food safety and so on. To use SHINERS in routine applications, a key problem is the development of functionalized and ultrathin shells to capture target molecules.

In this study, we exploited a novel fabrication method to fabricate ultrathin and compact Au@ poly (2-aminothiophenol) (PAT) nanoparticles (NPs) with good stability which were applicable in strong acid and alkaline solutions with pH from 2.02 to 12.95. By only adjusting the molar ratio of sodium dodecylsulfate (SDS) to

2-aminothiophenol, we were able to control the core-shell nanostructure shell thickness which can reach upto 2 nm and the shell was functionalized with amino groups *in situ*. Importantly, our aim is to provide an application platform for trinitrotoluene (TNT) explosive identification and detection based on the formation of Meisenheimer complexes between TNT and amino groups which come from the shells of Au@PAT NPs. As shown in Fig. 1, first of all, SDS was self-assembled onto the Au NP surface *via* electrostatic interactions; 2-aminothiophenol which contains a –SH group and an –NH₂ group should adsorb favorably onto Au NPs due to formation of Au–S bonds and the electrostatic affinity of the amino group to the colloidal gold. Coordination of SDS and 2-aminothiophenol molecules on Au NPs replaces the citrate ions. Polymerization subsequently proceeded followed by addition of (NH₄)₂S₂O₈.

To understand the influence of the SDS amount on the morphology of Au@PAT composites, a set of control experiments were performed with the molar ratios of SDS to 2-aminothiophenol ranging from 5 : 1 to 11 : 1, while the other synthetic parameters were kept constant. In this method, it was found that the molar ratio of SDS to 2-aminothiophenol (denoted by *X*) has significant impacts upon the PAT shell thickness. Fig. 2a–c present the TEM images of Au@PAT NPs with different PAT shell thicknesses from *ca.* 2 nm

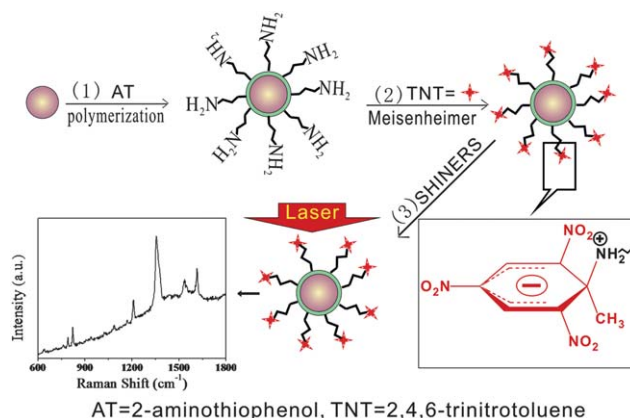


Fig. 1 The proposed procedure for the synthesis of a PAT shell coating an Au core and representation of the formation of a Meisenheimer complex between Au@PAT NPs and TNT. (1) Synthesis of amino-functionalized Au@PAT NPs through polymerization; (2) formation of a Meisenheimer complex in the presence of TNT; and (3) SHINERS detection of TNT.

Institute of Intelligent Machines, Chinese Academy of Sciences, Hefei 230031, China. E-mail: lbyang@iim.ac.cn; jhliu@iim.ac.cn; Fax: +86 551-5592420

† Electronic supplementary information (ESI) available: Detailed experimental procedures, additional figures of plots demonstrating SERS spectra in the presence of TNT (10–5 M), DDT, NP, NB and toluene (10–3 M). See DOI: 10.1039/c2an35947b

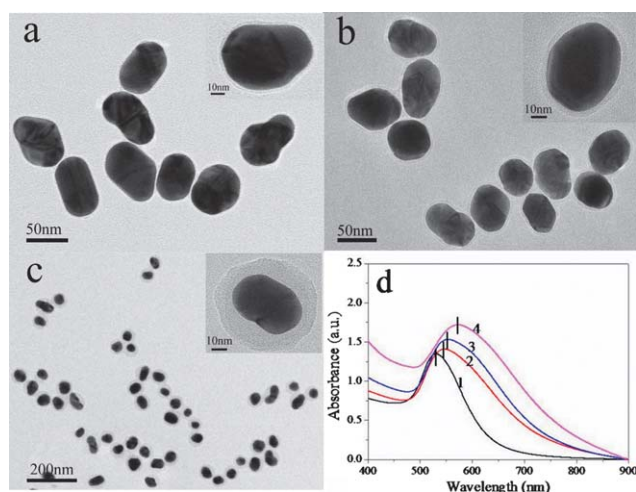


Fig. 2 (a–d) TEM images of Au/PAT core-shell nanoparticles with different shell thicknesses due to the different molar ratios of SDS to 2-aminothiophenol: (a) $X = 11 : 1$, 2 nm; (b) $X = 7 : 1$, 4 nm; (c) $X = 5 : 1$, 10 nm; and (d) absorption spectra of 50 nm Au@PAT NPs with different shell thicknesses from about 2 nm (curve 2), 4 nm (curve 3) up to 10 nm (curve 4) in comparison with that of bare ~ 50 nm Au NPs (curve 1).

($X = 11 : 1$), 4 nm ($X = 7 : 1$) up to 10 nm ($X = 5 : 1$) with decrease of X values, respectively. It was found that the increasing SDS concentration could decrease the layer thickness of the PAT on Au NPs. Apparently, SDS was in sufficient quantity to stabilize the excess PAT, preventing it from coagulating with the Au@PAT NPs. So it is very easy to form the ultrathin PAT shell when X is 11 : 1. Fig. 2d shows the absorption spectra of aqueous dispersions of Au@PAT colloids with different shell thicknesses from about 2, 4 to 10 nm. Before coating, the gold nanoparticles had a characteristic surface plasmon peak at ~ 530 nm (curve 1). When the surfaces of these gold nanoparticles were coated with PAT shells with thicknesses from 2, 4 to 10 nm, the plasmon peak was red shifted to 545 nm (curve 2), 552 nm (curve 3) and 572 nm (curve 4).

To prove the advantage of the Au@2 nm PAT NPs, we add weight to research its stability and applicable scope. Here we studied their resistance to acids and bases which we used, hydrochloric acid and sodium hydroxide solutions, to adjust pH. In Fig. 3a, when the pH was 6.86, the resulting solution appeared to be violet in color. The color of the products changed to lavender, dusty blue and gray when the pH decreased to 2.02, 1.85 and 1.70, respectively. When the pH increased to 12.95, 13.15 and 13.38, the color of the resulting solution also

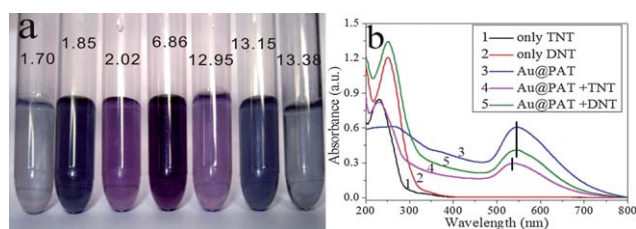


Fig. 3 (a) Photographic images of Au@2 nm PAT solutions with different pH values, from 1.70 to 1.85, 2.02, 6.86, 12.95, 13.15 and 13.38, respectively. (b) Absorption spectra of TNT (curve 1), DNT (curve 2) and Au@2 nm PAT (curve 3). Absorption spectral changes of Au@2 nm PAT NPs in the presence of 2.5×10^{-4} M TNT (curve 4). Absorption spectra remain the same in the presence of 2.5×10^{-4} M DNT (curve 5).

changed from lavender, dusty blue to gray. The change of the color may be because of the shell of PAT being destroyed in strong acid and alkaline media. Based on the above phenomenon, we could conclude that the Au@2 nm PAT NPs can be applicable in strong acid and alkaline solutions whose pH values were varied from 2.02 to 12.95.

TNT is a highly explosive and environmentally deleterious substance which has been of societal security concern, and therefore the exploration of detection and sensors for ultratrace TNT has attracted considerable research efforts recently.⁴ Our detection is based on the formation of Meisenheimer complexes between TNT and amino groups which come from the shells of Au@PAT NPs (as shown in the step (2) of Fig. 1). Since TNT is typically electron-deficient due to the strong electron-withdrawing effect of the nitro group, TNT is able to form Meisenheimer complexes even in the gas phase.⁵ Furthermore, Au@PAT NPs which have amino groups are electron-donating; so the electron-withdrawing analyte, TNT, readily reacts with electron-donating primary amino groups to form Meisenheimer complexes. UV-vis spectra (as shown in Fig. 3b) of the complex shows a new absorption band at 535 nm (curve 4) with a shift to the blue region in the presence of 0.25 mM TNT which suggested the formation of Meisenheimer complexes, compared with the Au@2 nm PAT solution whose absorption band was at 545 nm (curve 3). The observation of visible absorption clearly demonstrates that a strong molecular interaction occurs between the electron-deficient aromatic ring of TNT and the electron-rich amino group of Au@PAT NPs in the solution system. The TNT molecule is a Bronsted–Lowry acid and can be deprotonated at the methyl group by a basic amine. The negative charge on the TNT anion is distributed throughout the molecule through resonance stabilization by three electron-withdrawing nitro groups.⁶

To understand the structure of the Meisenheimer complex, we also performed SERS spectra of the Meisenheimer complex (shown in Fig. 4a). It clearly shows that a strong band appears around 2955 cm^{-1} for the Meisenheimer complex and it is due to the NH^{2+} symmetric stretching, C–H stretching and CH_2 asymmetric stretching.⁷ Fig. 4a shows the SERS spectra of 10^{-2} M to 10^{-5} M TNT, upon addition into Au@PAT NPs. The SERS spectra (as shown in Fig. 4a) exhibit several prominent TNT peaks. The strong Raman band at 1360 cm^{-1} is due to the NO_2 symmetric stretching vibration and the weak band at 1533 cm^{-1} is due to the NO_2 asymmetric stretching vibration. The peak at 1615 cm^{-1} is due to the C=C aromatic stretching vibration, all of them ($1360, 1533, 1615 \text{ cm}^{-1}$) are due to TNT vibration.⁸ And the band at 1422 cm^{-1} which corresponds to the N–H bending deformation band of the protonated amine belongs to Au@PAT.

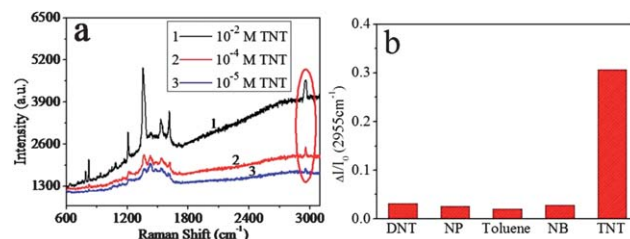


Fig. 4 (a) SERS spectra of Au@2 nm PAT NPs + TNT (10^{-2} M to 10^{-5} M) and the bands in the ellipse represent Meisenheimer complexes; (b) selectivity of Au@2 nm PAT NPs Raman enhancement relative intensity ($\Delta I/I_0$) to TNT and its structure-like molecules: dinitrotoluene (DNT), nitrophenol (NP), nitrobenzene (NB), toluene and TNT (I_0 represents the Raman intensity at 2955 cm^{-1} in the presence of analytes, respectively).

In summary, we present a facile one-step method to prepare Au/PAT core-shell nanoparticles which are uniform, free of pinholes and multifunctional with tunable shell thicknesses. Because the PAT shells were coated by multifunctional amino groups, in the presence of TNT, Au@PAT NPs can form Meisenheimer complexes and are the selective probe for TNT detection; so we expand the versatility of the shell which will open a wide scope of applications for SHINERS. The Au@PAT NPs may also be applicable to more general spectroscopy such as infrared spectroscopy, sum frequency generation and fluorescence. We believe that the nanocomposites would be a new class of SERS nanosensors allowing future practical applications in detection of target molecules or ions.

This work was supported by the National Basic Research Program of China (2011CB933700), Major national scientific instrument and equipment development project (2011YQ0301241001 and 2011YQ0301241101) and the Important Projects of Anhui Provincial Education Department (KJ2010ZD09).

Notes and references

- 1 J. F. Li, Y. F. Huang, Y. Ding, Z. L. Yang, S. B. Li, X. S. Zhou, F. R. Fan, W. Zhang, Z. Y. Zhou, D. Y. Wu, B. Ren, Z. L. Wang and Z. Q. Tian, *Nature*, 2010, **464**, 392–395.
- 2 (a) J. F. Li, S. B. Li, J. R. Anema, Z. L. Yang, Y. F. Huang, Y. Ding, Y. F. Wu, X. S. Zhou, D. Y. Wu, B. Ren, Z. L. Wang and Z. Q. Tian, *Appl. Spectrosc.*, 2011, **65**, 620–626; (b) J. R. Anema, J. F. Li, Z. L. Yang, B. Ren and Z. Q. Tian, *Annu. Rev. Anal. Chem.*, 2011, **4**, 129–150; (c) B. Liu, A. Blaszczyk, M. Mayor and T. Wandlowski, *ACS Nano*, 2011, **5**, 5662–5672; (d) J. F. Li, J. R. Anema, Y. C. Yu, Z. L. Yang, Y. F. Huang, X. S. Zhou, B. Ren and Z. Q. Tian, *Chem. Commun.*, 2011, **47**, 2023–2025; (e) J. F. Li, S. Y. Ding, Z. L. Yang, M. L. Bai, J. R. Anema, X. Wang, A. Wang, D. Y. Wu, B. Ren, S. M. Hou, T. Wandlowski and Z. Q. Tian, *J. Am. Chem. Soc.*, 2011, **133**, 15922–15925; (f) A. R. Guerrero and R. F. Aroca, *Angew. Chem., Int. Ed.*, 2011, **50**, 665–668.
- 3 D. Graham, *Angew. Chem., Int. Ed.*, 2010, **49**, 9325–9327.
- 4 (a) A. Rose, Z. G. Zhu, C. F. Madigan, T. M. Swager and V. Bulovic, *Nature*, 2005, **434**, 876–879; (b) T. L. Andrew and T. M. Swager, *J. Am. Chem. Soc.*, 2007, **129**, 7254–7255; (c) L. B. Yang, L. Ma, G. Y. Chen, J. H. Liu and Z. Q. Tian, *Chem.–Eur. J.*, 2010, **16**, 12683–12693.
- 5 J. Yinon, J. V. Johnson, U. R. Bernier, R. A. Yost, H. T. Mayfield, W. C. Mahone and C. Vorbeck, *J. Mass Spectrom.*, 1995, **30**, 715–722.
- 6 (a) N. R. Walker, M. J. Linman, M. M. Timmers, S. L. Dean, C. M. Burkett, J. A. Lloyd, J. D. Keelor, B. M. Baughman and P. L. Edmiston, *Anal. Chim. Acta*, 2007, **593**, 82–91; (b) C. F. Bernasco, *J. Org. Chem.*, 1971, **36**, 1671–1679.
- 7 S. S. R. Dasary, A. K. Singh, D. Senapati, H. T. Yu and P. C. Ray, *J. Am. Chem. Soc.*, 2009, **131**, 13806–13812.
- 8 (a) N. Gupta and R. Dahmani, *Spectrochim. Acta, Part A*, 2000, **56**, 1453–1456; (b) K. Kneipp, Y. Wang, R. R. Dasari, M. S. Feld, B. D. Gilbert, J. Janni and J. I. Steinfeld, *Spectrochim. Acta, Part A*, 1995, **51**, 2171–2175.